J Mater Sci (2013) 48:3511–3516
DOI 10.1007/s10853-013-7144-9

Reduced leakage current and enhanced ferroelectric properties in Mn-doped $Bi_{0.5}Na_{0.5}TiO_3$-based thin films

M. M. Hejazi · E. Taghaddos · A. Safari

Received: 6 December 2012 / Accepted: 5 January 2013 / Published online: 16 January 2013

Abstract $Bi_{0.5}(Na_{0.76}K_{0.2}Li_{0.04})_{0.5}TiO_3$ thin films were deposited on $SrRuO_3$-coated (001)-$SrTiO_3$ substrates by pulsed laser deposition. The effects of oxygen pressure and Mn doping on the leakage current and ferroelectric and dielectric properties were investigated. The remnant polarization and dielectric constant (at 10 kHz) of Mn-doped film deposited at 400 mtorr were measured to be 23 $\mu C\ cm^{-2}$ and 660, respectively. The leakage current density of Mn-doped films was suppressed by more than two orders of magnitude and the polarization was considerably enhanced. The XPS results showed coexistence of Mn^{2+}, Mn^{3+}, and Mn^{4+} in doped films. Oxidation of Mn^{2+} to higher valence states by absorbing holes along with occupation of A-site vacancies was suggested as the possible reason for a reduced leakage current and dielectric loss in Mn-doped films.

Introduction

Lead-free ferroelectric thin films have attracted a lot of attention during the past few years. However, compared to their lead-based counterparts, they suffer from inferior insulating properties. This is one of the main drawbacks facing the development of lead-free thin films for practical applications such as capacitors and memories in which low values of leakage current and dielectric loss are demanded. Recently, it has been demonstrated that the leakage current of lead-free films such as $K_{0.5}Na_{0.5}NbO_3$ (KNN) [1–3], $Bi_{0.5}Na_{0.5}TiO_3$ (BNT) [4–6], $BaTiO_3$ (BTO) [7], $NaNbO_3$ (NN) [8–10], and $BiFeO_3$ (BFO) [11] can be reduced by the addition of manganese. A literature survey, however, shows that there is a controversy in the published results on the effects of Mn on leakage current and dielectric properties. Some researchers have reported that Mn doping deteriorates the electrical properties of lead-free thin films and crystals [12–16]. Kawae et al. [11] indicated that the formation of deep traps by Mn doping decreased the leakage current of BFO thin films. Chung et al. [15], on the contrary, showed that Mn doping increased the leakage current and dielectric loss due the creation of oxygen vacancies. While Mn doping in KNN-based thin films remarkably enhanced the remnant polarization and suppressed the leakage current [1, 3, 17], it did not enhance the ferroelectric properties of KNN thick films [18]. The formation of oxygen vacancies acting as trapping centers in Mn-doped BTO thin films increased the dielectric loss at low frequencies [7]. On the other hand, Chu et al. [19] demonstrated that the dielectric loss was decreased considerably with Mn doping. A high concentration of Mn also deteriorates the electrical properties by formation of secondary phases [1, 20]. Differences in deposition techniques, microstructure, crystallographic orientation, compositional homogeneity, and defects may be responsible for the variation of results in the published literature. Thus, more research needs to be implemented to clarify the effects of Mn doping in lead-free materials.

Mn basically acts as an acceptor dopant replacing Ti^{4+} or Fe^{3+} in the perovskite structure and creates doubly ionized oxygen vacancies [14, 21]. It is believed that the fluctuation of Mn valence states is the key factor for decreasing the leakage current [9, 22]. On the other hand, the processing parameters, particularly the oxygen pressure, affect the concentration of intrinsic oxygen vacancies,

---

M. M. Hejazi (✉) · E. Taghaddos · A. Safari
Glenn Howatt Electroceramics Laboratories, Department of Materials Science and Engineering, Rutgers, The State University of New Jersey, Piscataway, NJ 08854, USA
e-mail: mmhejazi@eden.rutgers.edu; mm.hejazi@rutgers.edu

electronic defects, and the Mn oxidation state. Therefore, PO_2 during the growth, cooling, or post-annealing treatment is one of the most critical factors with which the effect of Mn doping is correlated [22]. In this paper, we report the influence of 2 mol.% Mn doping on the electrical properties of pulsed laser deposited (PLD) $Bi_{0.5}(Na_{0.76}K_{0.2}Li_{0.04})_{0.5}TiO_3$ (abbreviated to BNKLT76) thin films grown at two different oxygen pressures. The BNKLT76 composition is a morphotropic phase boundary (MPB) between rhombohedral and tetragonal phases, which exhibits relatively high values of piezoelectric charge coefficient ($d_{33} \sim 174$ pC N^{-1}), planar coupling coefficient ($k_p \sim 0.36$), and thickness coupling coefficient ($k_t \sim 0.52$) in the bulk form [23, 24] and can be regarded as a promising alternative for lead-based ceramics. A ferroelectric to antiferroelectric phase transition determines the depolarization temperature of this composition which is reported to occur at about 170 °C [24]. Despite comprehensive studies on ceramics with this MPB composition, there are no reports on the ferroelectric and dielectric properties of the thin films.

Experimental procedure

Undoped and 2 mol.% Mn-doped films (500 nm thick) with target composition of $Bi_{0.5}(Na_{0.76}K_{0.2}Li_{0.04})_{0.5}TiO_3$ were deposited on $SrRuO_3$-coated (001)-$SrTiO_3$ substrates by the PLD technique. A detailed explanation on preparation of ceramic targets can be found elsewhere [28]. Epitaxial films with (001) orientation were grown at a substrate temperature of 800 °C, laser repetition rate of 10 Hz, laser energy density of 1.2 J cm^{-2}, and oxygen pressures of 200 and 400 mtorr. Following the deposition, films were cooled down inside the PLD chamber at 1 atm oxygen pressure. Au electrodes of 200 μm in diameter were sputtered on top of the film for electrical properties' characterization. The ferroelectric and dielectric properties of the thin films were studied using an RT 66A ferroelectric test system (Radiant Inc.) and a LCR meter (HP4284A) at room temperature. The leakage current of the films was also measured by Precision LC (Radiant Inc.) equipment.

Results and discussion

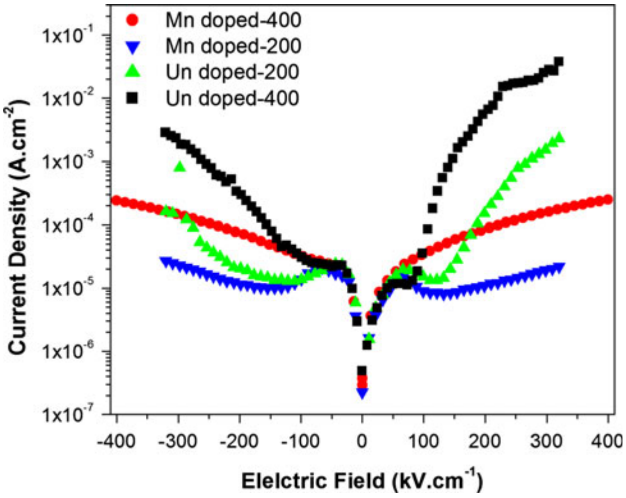

Fig. 1 Effect of Mn doping and oxygen pressure on the leakage current density of Au/BNKLT76/SRO heterostructures

Figure 1 shows the effects of oxygen pressure and Mn doping on the leakage current of BNKLT76 thin films measured at room temperature. Increasing the oxygen pressure from 200 to 400 mtorr in undoped films increased the leakage current density at 200 kV cm^{-1} from 1.5×10^{-4} to 5×10^{-3} A cm^{-2}. It can be observed that the Mn doping remarkably decreased the leakage current of both films deposited at different oxygen pressures. The leakage current density of the doped film prepared at 200 mtorr remained below 2×10^{-5} A cm^{-2} even at high electric fields, which is significantly lower than other undoped BNT-based thin films with MPB composition [25, 26]. The effect of Mn doping was particularly more pronounced in the film deposited at 400 mtorr in which the leakage current density at 300 kV cm^{-1} was decreased by more than two orders of magnitude. The reduction in leakage current is also in agreement with 0.5 mol.% Mn-doped BNT-BT thin films prepared by the PLD [5]. Wu et al. [20] reported that the addition of 2 mol.% Mn in BNT thin films prepared by sol–gel did not considerably decrease the leakage current, while increasing the concentration of Mn up to 6 mol.% suppressed the leakage current by one order of magnitude.

Due to the fact Mn is a multivalent element, it might be incorporated into the lattice under different valences such as Mn^{2+} ($r \sim 0.67$ Å low spin, $r \sim 0.83$ Å high spin), Mn^{3+} ($r \sim 0.58$ Å low spin, $r \sim 0.64$ Å high spin), and Mn^{+4} ($r \sim 0.53$ Å). Considering the ionic radii of different cations in the host lattice [Ti^{+4} ($r \sim 0.61$ Å), Bi^{3+} ($r \sim 1.03$ Å), Na^{+} ($r \sim 1.02$ Å), K^{+} ($r \sim 1.38$ Å), and Li^{+} ($r \sim 0.74$ Å)], Mn is expected to occupy the Ti cations located at the B-site. Therefore, Mn doping is accompanied by the formation of extrinsic oxygen vacancies to maintain the charge neutrality:

$$2Mn^{3+} = 2Mn'_{Ti} + V_O^{\bullet\bullet}, \quad (1a)$$

$$Mn^{2+} = Mn''_{Ti} + V_O^{\bullet\bullet}, \quad (1b)$$

where Mn'_{Ti} and Mn''_{Ti} represent Mn^{3+} and Mn^{2+}, respectively, at the Ti site and $V_O^{\bullet\bullet}$ denotes an oxygen vacancy.

In addition, the volatilization of A-site elements during the high temperature processing results in generating

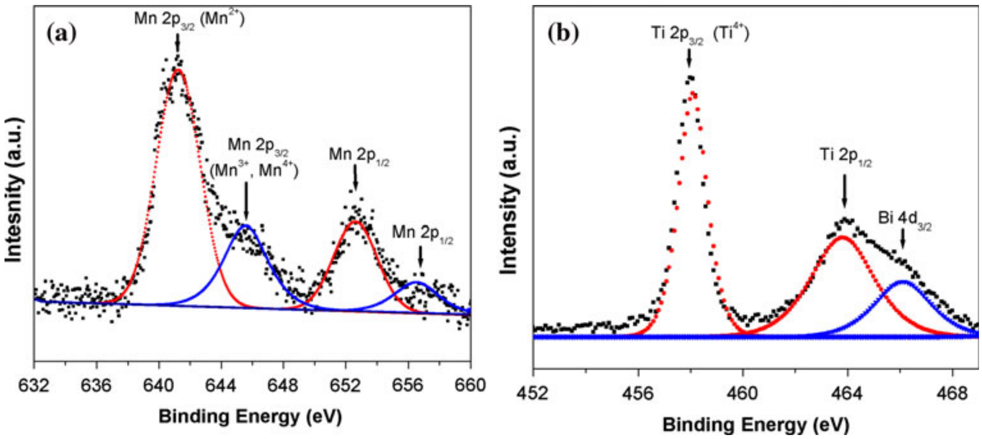

Fig. 2 **a** Mn 2p XPS spectrum of doped film prepared at 400 mtorr **b** Ti 2p XPS spectrum of undoped film deposited at 200 mtorr

intrinsic oxygen vacancies [9, 10, 27, 28] which compensate for the negatively charged A-site vacancies:

$$2\mathrm{Bi}_{\mathrm{Bi}}^{*} + 3\mathrm{O}_{\mathrm{O}}^{*} = 2\mathrm{V}_{\mathrm{Bi}}''' + 3\mathrm{V}_{\mathrm{O}}^{\bullet\bullet} + \mathrm{Bi_2O_3(g)}\uparrow, \qquad (2a)$$

$$2\mathrm{Na}_{\mathrm{Na}}^{*} + \mathrm{O}_{\mathrm{O}}^{*} = 2\mathrm{V}_{\mathrm{Na}}' + \mathrm{V}_{\mathrm{O}}^{\bullet\bullet} + \mathrm{Na_2O(g)}\uparrow. \qquad (2b)$$

Intrinsic and extrinsic oxygen vacancies can act as charge carriers leading to an increase in the leakage current, particularly at temperatures higher than room temperature [12, 27, 28]. They can also function as bridging connectors between B-site cations facilitating the electron hopping phenomenon which is a known source of electrical conduction in ferroelectric thin films with the perovskite structure [20].This is, however, in contradiction with the results obtained in this research as well as several other papers which show that Mn doping improves the insulating properties of perovskite thin films. It is believed that the oxygen vacancies have negligible contribution to the leakage current of thin films at room temperature. Furthermore, the possible formation of the defect complexes such as [$\mathrm{Mn}_{\mathrm{Ti}}'$–$\mathrm{V}_{\mathrm{O}}^{\bullet\bullet}$] and [$\mathrm{Mn}_{\mathrm{Ti}}''$–$\mathrm{V}_{\mathrm{O}}^{\bullet\bullet}$] [2, 29, 30] decreases the concentration of free oxygen vacancies. Nevertheless, oxygen vacancies indirectly increase the leakage current through formation of holes ($\mathrm{h}^{\bullet}$). Exposure of oxygen vacancies to an oxygen environment (during the deposition, cooling, or annealing steps) creates $\mathrm{h}^{\bullet}$ leading to a p-type conduction behavior:

$$\frac{1}{2}\mathrm{O}_2 + \mathrm{V}_{\mathrm{O}}^{\bullet\bullet} = \mathrm{O}_{\mathrm{O}}^{*} + 2\mathrm{h}^{\bullet}. \qquad (3)$$

These holes have higher mobility than oxygen vacancies and particularly deteriorate the insulating properties at room temperature [28]. As shown in Fig. 1, the leakage current of undoped and doped BNT-based thin films increased with oxygen pressure. According to Eq. 3, a higher oxygen pressure increases the concentration of holes, which in turn increases the leakage current of the films. In addition, the variation of the oxygen pressure during the deposition of thin films with the PLD process affects the stoichiometry of the films. On the one hand, increasing the oxygen pressure may thermodynamically hinder the volatilization of A-site elements by decreasing the equilibrium constant of the oxide dissociation. On the other hand, the kinetic energy of the species flying from the plasma plume toward the substrate decreases as the oxygen pressure increases. This momentum change, which is more significant for lighter elements along with a contraction in the plume size, may lead to the deposition of films with non-uniform chemical composition. The electrical properties of thin films, therefore, are a complex function of the oxygen pressure [31] which affects the chemical composition of the films as well as the defect structure.

The oxidation states of Mn and Ti were explored by X-ray photoelectron spectroscopy (XPS, Al K_{α}, K-Alpha, Thermoscientific) and the representative spectra are depicted in Fig. 2a, b.

Figure 2a shows the Mn $2p_{3/2}$ and Mn $2p_{1/2}$ XPS spectra in the Mn-doped film deposited at 400 mtorr. The peak observed at a binding energy of 641.2 eV corresponds to the divalent manganese cation. Since the Mn peaks of different oxidation states are located very close to each other, it is difficult to indicate the exact position for each valence state. However, the peak broadening of Mn $2p_{3/2}$ orbit at a binding energy of about 645 eV reveals the coexistence of Mn^{2+} with higher valence cations (Mn^{3+} and Mn^{4+}), which is similar to Mn-doped BFO thin films and KNN crystals [22, 30]. Using the peak fitting analysis, the ratio of Mn^{2+} to Mn^{3+} and Mn^{4+} was calculated to be about 3:1. The XPS spectrum of the doped film grown at 200 mtorr (not shown here) also exhibited the existence of mixed valence states for Mn. However, the relative amount of Mn^{2+} in this film was higher compared to the film deposited at 400 mtorr. It can be speculated that Mn divalent cations incorporated at the B-site can absorb holes [9, 10, 27]. As a result, Mn^{2+} can be oxidized to Mn^{+3} or Mn^{+4} according to the following equations:

$$\mathrm{Mn}''_{\mathrm{Ti}} + \mathrm{h}^{\bullet} = \mathrm{Mn}'_{\mathrm{Ti}}, \tag{4a}$$

$$\mathrm{Mn}'_{\mathrm{Ti}} + \mathrm{h}^{\bullet} = \mathrm{Mn}^{*}_{\mathrm{Ti}}. \tag{4b}$$

Manganese in BNT-based thin films, therefore, reduces the leakage current by limiting the contribution of the holes. This is consistent with the results of other Mn-doped thin films [5, 7, 9, 10, 20]. According to Fig. 1, the leakage current suppression was more pronounced in the film deposited at 400 mtorr, probably due to the fact that this film contained a higher concentration of holes compared to the sample prepared at 200 mtorr.

Although it is more probable that Mn ions replace the B-site of ABO_3 Perovskite structure [9, 20, 21, 27–29, 32], the possibility of the A-site occupation by Mn cannot be excluded [5, 33–35]. Since the ionic radii of Mn^{2+} and Mn^{3+} ions are also close to those of Bi^{3+}, Na^{+}, K^{+}, and Li^{+}, Mn can fill A-site vacancies created as a result of A-site volatilization. Therefore, it decreases the concentration of vacancies and hence declines the leakage current which is supported by the obtained data. It is shown that Mn addition improves the resistivity of BNT crystals, probably with the same proposed mechanism [35]. Simultaneous occupation of the A- and B-sites by Mn which induces both hard and soft characteristics has been reported for other materials such as KNN thin films [3]. As mentioned previously, one of the other origins of electrical conduction and dielectric loss in thin films and ceramics with the perovskite structure is the electron hopping through B-site cations of different valences such as Ti^{4+} and Ti^{+3} [20, 36, 37]. In BNT-based thin films deposited by the sol–gel technique, Mn doping decreased the leakage current by preventing the reduction of Ti^{+4}–Ti^{+3} [20, 36]. Fig. 2b illustrates the Ti 2p XPS spectrum for the undoped sample deposited at 200 mtorr, showing that Ti exists in form of Ti^{+4} ($2p_{3/2}$ peak appearing at 457.5 eV). The same valence state of Ti was also found in other films (not shown here). Since there was no indication of the Ti^{3+} existence in undoped films, the electron hopping could not be considered as a dominant mechanism of electrical conduction in these thin films.

Figure 3 shows the polarization–electric field (P–E) hysteresis loops for undoped and Mn-doped thin films measured by an RT66A ferroelectric test system (Radiant Inc.) at 1 kHz. It was found that Mn doping remarkably enhanced the ferroelectric polarization of the samples, which was in agreement with other reports [5, 20, 38, 39].

The remnant polarization (P_r) and saturation polarization also increased with increasing the oxygen pressure. The P_r in undoped films increased from 10.3 to 17.3 μC cm^{-2} as the oxygen pressure changed from 200 to 400 mtorr. After Mn addition, the P_r of the films prepared at 200 and 400 mtorr was enhanced by 80 and 35 %, respectively. The highest P_r (23 μC cm^{-2}) is achieved for the Mn-doped sample deposited at 400 mtorr. The enhancement of the remnant polarization by Mn doping can be explained through distortion of TiO_6 octahedra [40–42] and the increased tetragonality [5, 30] when Mn replaces the B-site cations. Mn substitution may increase the dipole size by lengthening the off-center displacement in the perovskite structure, and hence the polarization is improved. In BNT single crystals, the Mn doping results in an in-phase octahedral tilting [43] and it increases the ordering of polar nanoregions [34, 43], which in turn enhances the ferroelectric and dielectric properties and decreases the leakage current and dielectric loss [35, 44]. The reduced leakage current also played a role in the enhancement of polarization by increasing the effective applied electric field. Mn doping was found to increase the coercive field of thin films which is a common effect of B-site acceptor substitution and is also observed in Mn-doped KNN-based thin films [3]. The pining of the domain walls by oxygen vacancies and the alignment of defect dipoles in the direction of the applied electric field caused an increase in the coercive field in Mn-doped thin films.

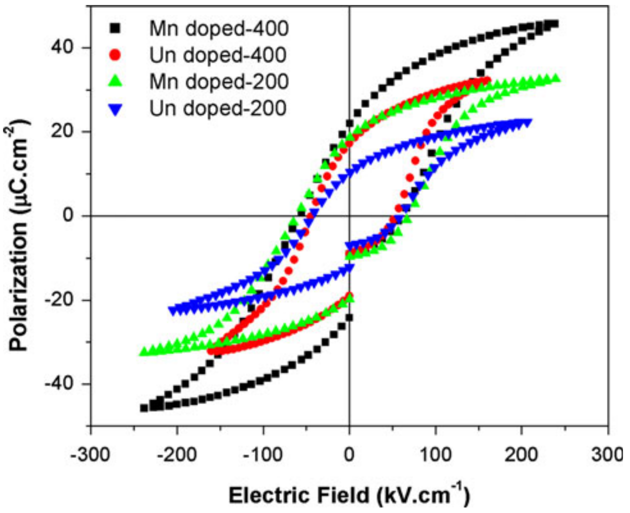

Fig. 3 P–E hysteresis loops of doped and undoped thin films deposited at 200 and 400 mtorr measured at 1 kHz

The dielectric constant and the dielectric loss of the films were measured as a function of frequency as depicted in Fig. 4. The dielectric properties showed a relaxation-type behavior as the loss tangent monolithically increased and relative permittivity decreased with frequency. Increasing the oxygen pressure increased the dielectric loss and the permittivity, which was in agreement with the leakage current data. The dielectric constant of undoped films at 10 kHz was enhanced from 470 to 690 by increasing the oxygen pressure. It was noticeable that the dielectric loss was effectively decreased by Mn doping.

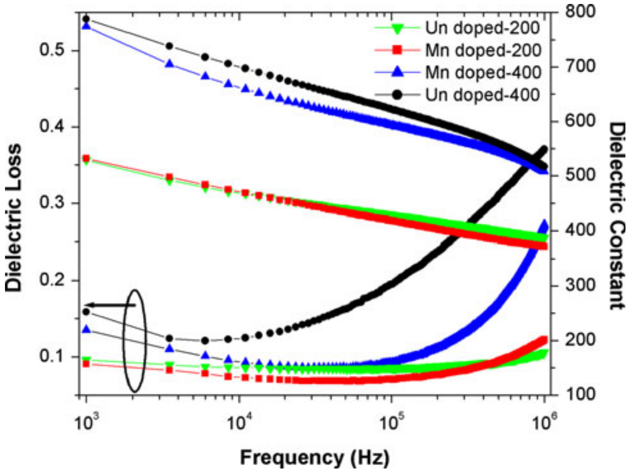

Fig. 4 Dielectric constant and dielectric loss as a function of frequency for Mn-doped and undoped films grown at 200 and 400 mtorr

Similar to the leakage current behavior, the influence of Mn doping in improvement of the dielectric loss was more noticeable for the film deposited at 400 mtorr. The dielectric loss at 10 kHz for samples deposited at 200 and 400 mtorr decreased from 0.09 to 0.07 and 0.14 to 0.1, respectively, through Mn doping. Despite decreasing the loss tangent, Mn doping did not degrade the dielectric constant as illustrated in Fig. 4. The dielectric constant of the doped film was close to that of the undoped film at 200 mtorr, while the dielectric constant of the 400 mtorr film just decreased by <8 % after Mn doping. A decrease in dielectric loss and relative permittivity with Mn addition has also been observed in BNT–BKT thick films [6]. Improvement in dielectric properties can be attributed to the effects of Mn on the concentration of defects, lattice distortion, and formation of defect complexes [2] as discussed previously.

In conclusion, Mn doping can be regarded as an effective method for suppression of the leakage current and dielectric loss in BNT-based thin films deposited by the PLD technique. It is speculated that Mn substitutes both the A- and B-sites of the perovskite structure and enhances the ferroelectric polarization of the films by the distortion of the TiO_6 octahedra and compensating for the charge carriers. The leakage current was shown to increase by increasing the oxygen pressure due to the formation of holes. Mn divalent cations can annihilate the generated holes via oxidation to higher valence states, which is confirmed by the XPS results. It is suggested that Mn probably occupies the A-site vacancies, which is another reason for the reduced leakage current observed in the doped thin films. Despite decreasing the loss tangent, Mn did not degrade the dielectric constant of the films. Mn-doped $Bi_{0.5}(Na_{0.76}K_{0.2}Li_{0.04})_{0.5}TiO_3$ thin films with a relatively high remnant polarization and dielectric constant can be considered as potential candidates for replacement of the lead-based ferroelectric counterparts.

Acknowledgements The financial support of this work by the Glenn Howatt Foundation is sincerely appreciated.

References

1. Kondo N, Sakamoto W, Lee B-Y, Iijima T, Kumagai J, Moriya M, Yogo T (2010) Jpn J Appl Phys 49(9):09MA04. doi:10.1143/jjap.49.09ma04
2. Fu F, Shen B, Zhai J, Xu Z, Yao X (2012) Ceram Int 38:S287. doi:10.1016/j.ceramint.2011.04.103
3. Abazari M, Safari A (2009) J Appl Phys 105(9):094101. doi:10.1063/1.3120922
4. Wu Y, Wang X, Zhong C, Li L (2011) J Am Ceram Soc 94(6):1843. doi:10.1111/j.1551-2916.2010.04325.x
5. Wang DY, Chan NY, Li S, Choy SH, Tian HY, Chan HLW (2010) Appl Phys Lett 97(21):212901. doi:10.1063/1.3518484
6. Zhang H, Jiang S, Kajiyoshi K (2009) J Am Ceram Soc 92(9):2147. doi:10.1111/j.1551-2916.2009.03166.x
7. Shuai Y, Zhou S, Buerger D, Reuther H, Skorupa I, John V, Helm M, Schmidt H (2011) J Appl Phys 109(8):084105. doi:10.1063/1.3576125
8. Sakamoto W, Hamazaki Y-i, Maiwa H, Morioka H, Saito K, Moriya M, Yogo T (2011) J Cryst Growth 318(1):879. doi:10.1016/j.jcrysgro.2010.11.054
9. Hamazaki Y-i, Sakamoto W, Moriya M, Yogo T (2009) Jpn J Appl Phys 48(9):09KA08. doi:10.1143/jjap.48.09ka08
10. Sakamoto W, Hamazaki Y-i, Maiwa H, Moriya M, Yogo T (2010) Thin Solid Films 518(15):4256. doi:10.1016/j.tsf.2009.12.102
11. Kawae T, Terauchi Y, Tsuda H, Kumeda M, Morimoto A (2009) Appl Phys Lett 94(11):112904. doi:10.1063/1.3098408
12. Singh SK, Ishiwara H (2006) Solid State Commun 140(9–10):430. doi:10.1016/j.ssc.2006.09.022
13. Pei L, Li M, Liu J, Yu B, Wang J, Guo D, Zhao X (2010) J Sol-Gel Sci Techn 53(2):193. doi:10.1007/s10971-009-2077-0
14. Chishima Y, Noguchi Y, Kitanaka Y, Miyayama M (2010) IEEE Trans Ultrason Ferr 57(10):2233. doi:10.1109/tuffc.2010.1683
15. Chung CF, Lin JP, Wu JM (2006) Appl Phys Lett 88(24):242909. doi:10.1063/1.2214138
16. Voisard C, Damjanovic D, Setter N (1999) J Eur Ceram Soc 19(6–7):1251. doi:10.1016/s0955-2219(98)00414-2
17. Abazari M, Choi T, Cheong SW, Safari A (2010) J Phys D Appl Phys 43(2):025405. doi:10.1088/0022-3727/43/2/025405
18. Han G, Priya S, Ryu J, Yoon W-H, Choi J-J, Hahn B-D, Park D-S (2011) Mater Lett 65(2):278. doi:10.1016/j.matlet.2010.09.077
19. Chu JP, Mahalingam T, Liu CF, Wang SF (2007) J Mater Sci 42(1):346. doi:10.1007/s10853-006-1032-5
20. Wu Y, Wang X, Zhong C, Li L (2011) J Am Ceram Soc 94(11):3877. doi:10.1111/j.1551-2916.2011.04576.x
21. Hayashi K, Ando A, Hamaji Y, Sakabe Y (1998) Jpn J Appl Phys Pt 1 37(9B):5237. doi:10.1143/jjap.37.5237
22. Noguchi Y, Miyayama M (2010) J Ceram Soc Jpn 118(1380):711
23. Hejazi M, Jadidian B, Safari A (2012) IEEE Trans Ultrason Ferroelectr Freq Control 59(8):1840
24. Hiruma Y, Nagata H, Takenaka T (2007) IEEE Trans Ultrason Ferr 54(12):2493. doi:10.1109/tuffc.2007.566
25. Hejazi MM, Safari A (2011) J Appl Phys 110(10):103710. doi:10.1063/1.3660428
26. Hejazi MM, Safari A (2011) J Adv Dielectr 1(1):57. doi:10.1142/S2010135X11000070

27. Noguchi Y, Yamamoto K, Kitanaka Y, Miyayama M (2007) J Eur Ceram Soc 27(13–15):4081. doi:10.1016/j.jeurceramsoc.2007.03.104
28. Noguchi Y, Matsumoto T, Miyayama M (2005) Jpn J Appl Phys Pt 2 44(16–19):L570. doi:10.1143/jjap.44.l570
29. Aksel E, Jakes P, Erdem E, Smyth DM, Ozarowski A, van Tol J, Jones JL, Eichelw R-A (2011) J Am Ceram Soc 94(5):1363. doi:10.1111/j.1551-2916.2010.04249.x
30. Huang J-Z, Wang Y, Lin Y, Li M, Nan CW (2009) J Appl Phys 106(6):063911. doi:10.1063/1.3225559
31. Hejazi M, Jadidian B, Safari A (2012) IEEE Trans Ultrason Ferr 59(9):1855. doi:10.1109/TUFFC.2012.2396
32. Kakimoto K, Masuda I, Ohsato H (2004) Jpn J Appl Phys Pt 1 43(9B):6706. doi:10.1143/jjap.43.6706
33. Nagata H, Takenaka T (2001) J Eur Ceram Soc 21(10–11):1299. doi:10.1016/s0955-2219(01)00005-x
34. Yao J, Ge W, Yan L, Reynolds WT, Li J, Viehland D, Kiselev DA, Kholkin AL, Zhang Q, Luo H (2012) J Appl Phys 111(6):064109. doi:10.1063/1.3699010
35. Ge W, Li J, Viehland D, Luo H (2010) J Am Ceram Soc 93(5):1372. doi:10.1111/j.1551-2916.2009.03551.x
36. Yuan Z, Lin Y, Weaver J, Chen X, Chen CL, Subramanyam G, Jiang JC, Meletis EI (2005) Appl Phys Lett 87(15):152901. doi:10.1063/1.2089181
37. Wu S, Wang S, Chen L, Wang X (2008) J Mater Sci-Mater El 19(6):505. doi:10.1007/s10854-007-9371-9
38. Zhong XL, Wang JB, Liao M, Tan CB, Shu HB, Zhou YC (2008) Thin Solid Films 516(23):8240. doi:10.1016/j.tsf.2008.03.004
39. Zhang Q, Whatmore RW (2003) J Appl Phys 94(8):5228. doi:10.1063/1.1613370
40. Huang J-Z, Shen Y, Li M, Nan C-W (2011) J Appl Phys 110 (9). doi:10.1063/1.3650460
41. Zhang ST, Chen YF, Wang J, Cheng GX, Liu ZG, Ming NB (2004) Appl Phys Lett 84(18):3660. doi:10.1063/1.1738936
42. Hu ZS, Zhong XL, Wang JB, Liao M, Zheng XJ, Zhou YC (2009) Surf Rev Lett 16(1):153
43. Yao JJ, Yang YD, Monsegue N, Li YX, Li JF, Zhang QH, Ge WW, Luo HS, Viehland D (2011) Appl Phys Lett 98(13):132903. doi:10.1063/1.3573801
44. Zhang QH, Zhang YY, Wang FF, Wang YJ, Lin D, Zhao XY, Luo HS, Ge WW, Viehland D (2009) Appl Phys Lett 95(10):102904. doi:10.1063/1.3222942